Isı Bilimi ve Tekniği Dergisi, 37, 2, 89-95, 2017
J. of Thermal Science and Technology

ISSN 1300-3615

# NUMERICAL ANALYSIS OF PULSATING CIRCULAR IMPINGING LAMINAR JET ON A PLANAR DISC

**Mitra KAHROBA* and Hasmet TÜRKOĞLU****

*Mechanical Engineering Department, Faculty of Engineering, Gazi University, Ankara, Turkey
**Corresponding author: Mechanical Engineering Department, Faculty of Engineering, Çankaya University, Ankara, Turkey, hasmet@cankaya.edu.tr

(Geliş Tarihi: 26.07.2016, Kabul Tarihi: 16.02.2017)

**Abstract:** In this study, the flow and heat transfer characteristics of pulsating circular air jets impinging on a flat surface were numerically analyzed. The jet velocity pulsated in time. The objective of the work is to investigate the influence of the jet Reynolds number, pulsation amplitude and pulsation frequency on the rate of heat transfer from the target hot surface. For the analysis, a computer program, based on the control volume method and SIMPLE algorithm, was developed. Laminar flow with the time averaged jet Reynolds numbers between 300 and 700 were analyzed. The pulsation amplitude is ranged between $0.0V_0$ (steady jet) and $0.8V_0$ (m/s) ($V_0$ is period averaged jet velocity), and the frequency is ranged between 1 and 6 Hz. The nozzle-to-plate distance was kept constant at H/d=3. From the simulation results, it was observed that at any instant of the pulsation period, the local Nusselt number is maximum at the stagnation point, and it decreases along the plate. This decrease in the local Nusselt number is not monatomic as in the steady jet cases. It has local maximum and minimum values (fluctuations) due to the moving recirculating flow regions along the bottom plate. At low frequencies, the time (period) averaged stagnation point Nusselt numbers are lower than the corresponding steady jet Nusselt numbers. However, with the increasing frequency, the stagnation point Nusselt number increases and become higher than the steady jet Nusselt number.
**Keywords:** Impinging jet; Pulsating jet; Numerical solution.

# DÜZLEM BİR DİSKE ÇARPAN OSİLASYONLU DAİRESEL LAMİNAR JETİN SAYISAL OLARAK İNCELENMESİ

**Özet:** Bu çalışmada, düzlem bir diske çarpan dairesel osilasyonlu jetlerin akış ve ısı transferi karakteristikleri sayısal olarak incelenmiştir. Çalışmanın amacı, dairesel bir nozuldan çıkıp düzlem bir yüzeye çarpan salınımlı hava jetinin, Reynolds sayısının, salınım genliğinin ve salınım frekansının, hedef yüzeyden akışkana olan ısı transferine etkilerini incelemektir. Bu sayısal çalışmayı yapmak için, kontrol hacmi formülasyonu ve SIMPLE algoritmasına dayanan bir bilgisayar programı geliştirilmiştir. Simülasyonlar, Reynolds sayısı 300 - 700, salınım genliği $0.0V_0$-$0,8V_0$ ve salınım frekansı 1-6 Hz aralığındaki jet akışlar için yapılmıştır. Nozul-çarpma yüzeyi arasındaki uzaklığın, lüle çapına oranı *H/d=3* sabit tutulmuştur. Simülasyon sonuçlarından çarpma periyodunun bütün anlarında durma noktası Nusselt sayısının maksimum olduğu ve durma noktasından uzaklaştıkça Nusselt sayısının azaldığı görülmüştür. Nusselt sayısındaki bu azalma, kararlı jetlerde olduğu gibi monotomik olmayıp yerel maksimum ve minum değerlere sahip olduğu gözlenmiştir. Alt levha üzerinde hareketli akış döngüleri meydana geldiği ve bu döngüler nedeniyle Nusselt sayısında yerel maksimum ve minimum değerlerin oluştuğu görülmüştür. Düşük salınım frekanslarında, Nusselt sayısı aynı Reynolds sayısına sahip kararlı jet Nusselt sayısından daha küçük olduğu, ancak artan frekansla salınımlı jet Nusselt sayısının arrtığı ve kararlı jet Nusselt sayısından daha yüksek değere ulaştığı görülmüştür.
**Anahtar Kelimeler:** Çarpan jet, Salınımlı jet, Sayısal çözüm.

## NOMENCLATURE

| | |
|---|---|
| A | Pulsation amplitude |
| $C_p$ | Specific heat of air, [J/kgK] |
| D | Diameter of the disc, [m] |
| d | Jet diameter, [m] |
| f | Pulsation frequency, [Hz] |
| h | Heat transfer coefficient at the target surface, [W/m$^2$K] |
| H | Nozzle-plate spacing, [m] |
| k | Thermal conductivity of air, [W/mK] |
| $Nu_{max}$ | Instantaneous stagnation point Nusselt number |
| $Nu_r$ | Instantaneous local Nusselt number |
| $N\bar{u}$ | Area and time averaged Nusselt number along the period |
| $N\bar{u}_A$ | Instantaneous area averaged Nusselt number |
| $N\bar{u}_{max}$ | Time averaged stagnation point Nusselt number |
| p | Pressure, [Pa] |
| Re | Reynolds number (Re= $V_o$ d/ν) |

$T_{in}$ Temperature of fluid at nozzle exit, [K]
$T_H$ Temperature of bottom plate, [K]
$q''$ Heat flux, [$W/m^2$]
$v_r$ Velocity component in radial- direction, [m/s]
$v_z$ Velocity component in axial- direction, [m/s]
$V_o$ Period averaged jet velocity, [m/s]
r Radial coordinate, [m]
z Axial coordinate, [m]

**Greek Symbols**

$\Delta t$ Computational time step, [s]
$\alpha$ Thermal diffusivity of fluid, [$m^2/s$]
$\rho$ Fluid density, [$kg/m^3$]
$\tau$ Period of pulsation, [s]
$\nu$ Kinematic viscosity, [$m^2/s$]

## INTRODUCTION

Impinging jets are widely used to enhance the heat and mass transfer from surfaces. The widespread usage of impinging jets in cooling and drying applications is attributed to their inherent superior performance over other schemes of single phase heat and mass transfer from a comparatively small surface area. Impinging jets are also used in chemical vapor deposition (CVD) processes.

The flow structure of an impinging jet over a planar target can be divided into three characteristic regions as free jet region, stagnation flow region and wall jet region. The free jet region is formed upon the jet exit with a defined velocity distribution as a function of the jet radius. A shear layer is generated due to the velocity difference between the potential core of the jet and the ambient fluid. However, there is not enough distance for the jet flow to mix with the surrounding fluid in the cases that the distance of jet exit-to-the target wall is short, as in the current study. The stagnation flow region results from the jet impact on the target solid surface. The wall jet region is formed because of re-acceleration of the flow along the target surface. The main part of heat transfer occurs in the proximity of the stagnation point, but a portion of the wall jet region may significantly contribute to the heat exchange, too. In spite of the simple geometry of the jet-plate combination, convective heat transfer coefficient at the target surface is affected by a variety of parameters such as the nozzle to plate distance, Reynolds number (Re), nozzle inclination angle, steadiness of the jet flow, etc.

From the literature review, it is deduced that unsteadiness of the jet flow has been rarely investigated. Studies about the influence of unsteady jet flow on the heat transfer rate via generating a periodic variation in the jet speed are accomplished (Zumbrunnen and Aziz, 1993; Azevedo et al, 1994; Miladin and Zumbrunnen, 1997; Liu and Sullivan, 1996]. These studies showed that there is no general trend about the effect of jet unsteadiness on the heat transfer rate, as some researchers found enhanced heat transfer and some do not.

Some researches show significant differences between flow fields with and without unsteady motions. According to existing data, the jets with unsteady velocity show strong mixing of the jet with ambient fluid and hence a rapid reduction in the maximum jet velocity. Considering this phenomenon as a positive result of unsteadiness on heat transfer rate due to the boundary layer renewal in stagnation region, the influence of unsteadiness on the heat transfer rate depends on various parameters. Goppert et al. (2004) pointed out that a threshold-frequency often exists above which the heat transfer augmentation occurs in general. It is obvious from the studies about impinging jets with low jet-to-plate distance normalized by the jet diameter (H/D) that the wall jet undergoes a transition to turbulence, but the mixing turbulence resulted from entrainment doesn't penetrate to the free jet center. Therefore, the stagnation Nusselt number is locally minimum at H/D=2 which is observed by Goldstein and Timmers (1982). Collucci and Viskanta (1996) also reported examples of a couple of Nusselt number peaks. The peak closer to the jet center is due to the thinning of the laminar boundary layer and the secondary one is because of the transition from laminar to turbulent flow in the wall jet. Study by Liu and Sullivan (1996) surveyed the fluctuating heat exchange to an impinging air jet excited acoustically. It was shown that excitation of the jet at certain frequencies leads to enhancement or reduction in both local and area averaged heat transfer. O'Donovan and Murray (2008) have observed the frequency bands growing within the transition region and diminishing as the wall jet transition to the turbulence. They also reported the variation of heat transfer rate as a result of periodic behavior of the flow in the wall jet region.

Demircan and Turkoglu (2010) investigated laminar sinusoidally oscillating rectangular impinging air jet on a planar surface for low Reynolds numbers and observed that the heat transfer increases with increasing Reynolds number and fluctuation amplitude and decreasing H/W ratio where W is width of the rectangular nozzle used in their work. As a result, it was concluded that the optimum values of H/W ratio and oscillation amplitude should be found to make heat transfer maximum.

The focus of the present study is to analyze how convective heat transfer is affected by the unsteady jet velocity. To do this, pulsating circular air jets impinging on a flat surface were numerically analyzed. The jet velocity is pulsated in time. For the analysis, a computer program, based on the control volume method and SIMPLE algorithm, was developed. The objective of the work is to investigate the influence of the jet Reynolds number, pulsation amplitude and pulsation frequency on the rate of heat transfer from the target hot surface.

## DESCRIPTION OF THE PROBLEM AND THE MATHEMATICAL FORMULATION

Two parallel, horizontal, infinite planar discs were considered in this study. The geometry of the problem and coordinate system considered are shown in Fig. 1. A pulsating air jet issuing from a circular hole at the center of the upper disc impinges on the bottom disc. The upper disc was insulated and the lower one is kept at constant temperature $T_H$ that is higher than the jet inlet temperature $T_{in}$.

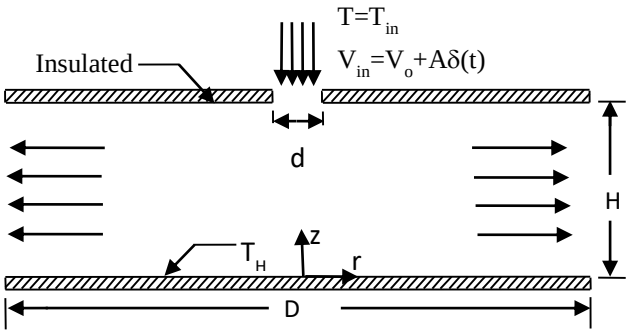


**Figure 1.** The geometry and the coordinate system of the problem.

The jet velocity over the nozzle exit is uniform but it varies with time periodically according to the function given by Eq. (1) below.

$$V_{in} = V_0 + A\delta(t) \tag{1}$$

where $V_0$ is the period averaged jet velocity and $A$ is the pulsation amplitude based on the average velocity $V_0$. $\delta(t)$ is the Dirac function which has a value as

$$\delta(t) = \begin{cases} 1 & \text{for } 0 < t \le \tau/2 \\ -1 & \text{for } \tau/2 < t < \tau \end{cases}$$

where $\tau$ is the pulsation period. It is assumed that the flow is laminar and incompressible. Since the temperature difference in the flow field is small, the variation in the fluid properties such as density, viscosity and heat conduction coefficient are assumed to be negligible. Also, the variations in all variables in the angular direction can be neglected. So, the basic equations of the problem in cylindrical coordinate system can be written as follows:

### Continuity Equation

$$\frac{1}{r}\frac{\partial}{\partial r}(r v_r) + \frac{\partial}{\partial z}(v_z) = 0 \tag{2}$$

### Conservation of linear Momentum Equations

In the axial direction (z-direction):

$$\rho\left(\frac{\partial v_z}{\partial t} + v_r\frac{\partial v_z}{\partial r} + v_z\frac{\partial v_z}{\partial z}\right) = -\frac{\partial p}{\partial z} + \mu\left[\frac{1}{r}\frac{\partial}{\partial r}\left(r\frac{\partial v_z}{\partial r}\right) + \frac{\partial^2 v_z}{\partial z^2}\right] \tag{3}$$

In radial direction (r-direction):

$$\rho\left(\frac{\partial v_r}{\partial t} + v_r\frac{\partial v_r}{\partial r} + v_z\frac{\partial v_r}{\partial z}\right) = -\frac{\partial p}{\partial r} + \mu\left[\frac{1}{r}\frac{\partial}{\partial r}\left(r\frac{\partial v_r}{\partial r}\right) + \frac{\partial^2 v_r}{\partial z^2}\right] \tag{4}$$

### Energy equation

$$\rho c_p\frac{\partial T}{\partial t} + \rho c_p v_z\frac{\partial T}{\partial z} + \rho c_p v_r\frac{\partial T}{\partial r} = k\left[\frac{1}{r}\frac{\partial}{\partial r}\left(r\frac{\partial T}{\partial r}\right) + \frac{\partial^2 T}{\partial z^2}\right] \tag{5}$$

### Boundary Conditions

The fluid temperature at nozzle outlet $T_{in}$ is constant and the vertical component of velocity is defined by the expression $V_{in} = V_0 + A\delta(t)$. The flow is assumed to be symmetric about the nozzle axis. The upper disc is insulated and the lower disc is kept at a prescribed constant temperature, $T_H$. On the solid surfaces no-slip condition applies and hence the velocity components are zero. At the surface, at $r=D/2$, through which the fluid leaves the flow domain, the variations of the velocity components and temperature were neglected.

### Calculation of Nusselt Number

The temperature and velocity fields vary with the time and the position in the flow domain. Hence, to characterize the heat transfer rate from the bottom plate, instantaneous local, instantaneous area averaged, area and time (period) averaged, instantaneous stagnation and time (period) averaged stagnation point Nusselt numbers are calculated. For the definition of these Nusselt numbers, Nozzle diameter d is considered as the characteristic length. The calculation of all these five different Nusselt numbers is formulated below.

The temperature distribution obtained by the numerical solution of the energy equation is used to calculate the Nusselt number along the hot bottom plate. The local instantaneous heat flux from the hot bottom plate to the fluid can be expressed as;

$$q'' = h(T_H - T_{in}) = -k\left.\frac{\partial T}{\partial z}\right)_{z=0} \tag{6}$$

In this equation, $T_H$ and $T_{in}$ are temperatures at the bottom wall and jet inlet, respectively. From this equation, the instantaneous local Nusselt number can be determined. Using the nozzle diameter $d$ as the characteristic length, the above equation can be rearranged as,

$$Nu_r = \frac{hd}{k} = -\frac{d}{(T_H - T_{in})}\left.\frac{\partial T}{\partial z}\right)_{z=0} \tag{7}$$

The instantaneous area averaged Nusselt number on the hot bottom plate can be calculated by integrating the

instantaneous local Nusselt number over the bottom surface.

$$\overline{Nu}_A = \frac{1}{A}\int_A Nu_r \, dA \tag{8}$$

The area and time averaged Nusselt number along the period of injection can be calculated by integrating Eq. (8) over the injection period τ.

$$\overline{Nu} = \frac{1}{\tau}\int_\tau \frac{1}{A}\int_A Nu_r \, dA dt \tag{9}$$

where $A$ is the area of the target surface and τ is the period of the pulsation. The instantaneous local Nusselt number at the stagnation point is equal to the Nusselt number at $r=0$ and it is the maximum Nusselt number. Hence, it can be expressed as

$$Nu_{\max} = Nu_r)_{r=0} \tag{10}$$

The period averaged stagnation point Nusselt number is calculated by integrating the instantaneous stagnation point Nusselt number along the period of injection as,

$$(\overline{Nu})_{\max} = \frac{1}{\tau}\int_\tau Nu_{\max} dt \tag{11}$$

## NUMERICAL SOLUTION

The continuity, momentum and the energy equations have to be solved together with the relevant boundary conditions to determine the velocity and temperature distributions in the flow field. These equations are linked with each other. Hence, the solution of this set of equations is only possible by using a numerical method. The numerical method used in this study is based on the control volume approach and SIMPLE algorithm. The governing equations were discretized by integrating them over finite control volumes. The hybrid scheme was used for the discretization. The time dependent terms were discretised using the fully implicit scheme. Gauss-Seidel iteration technique was used for solving the algebraic equations. A computer program developed in our one of previous study was modified to solve the present problem. Using the computer program developed, the velocity, pressure and temperature distributions were obtained for all grid points at different instants of the injection period.

To minimize the numerical errors and optimize the solution time, a non-uniform grid system was used. Near the top and bottom plates and also around the axis of the jet, finer grid spacing was utilized. To determine the optimum size of the mesh, by keeping all other parameter constant, the simulation of the problem was repeated with different grid systems and time steps. Comparing the area averaged and stagnation point Nusselt numbers obtained with different mesh sizes and time steps, the optimum mesh size and time step were determined.

To obtain periodically fully developed results, the computations were repeated successively until the difference between Nusselt numbers for two successive periods is negligibly small. The validity of the numerical scheme and the computer program used in this study was checked by Demircan and Turkoglu (2010) in a previous study. Based on the comparison of the results obtained using the computer program developed with the results in the literature, it was shown that the developed model and computer code simulate the unsteady impinging jet flow and heat transfer with a satisfactory accuracy.

## RESULTS AND DISCUSSIONS

In this study, the heat transfers and flow characteristics of impinging air jets which have a periodically pulsating velocity in time were analyzed. The jet velocity was changed according to the expression given by Eq. (1). In Fig. 2, the variations of the jet velocity along the pulsation period are shown for different pulsation amplitudes. As seen in this figure, during the first half of the injection period, the jet velocity is at its maximum value, and during the second half of the pulsation period, the jet velocity assumes its minimum value. Computations were performed for different Reynolds numbers ($Re=V_0 d/\nu$=100, 300, 500 and 700), the jet velocity amplitudes (A=0.2$V_0$, 0.4$V_0$, 0.6$V_0$ and 0.8$V_0$) and the jet oscillation frequencies ($f$=1 Hz, 2 Hz, 3 Hz, 4 Hz, 5 Hz and 6 Hz) with fixed geometrical dimensions of $H/d$=3 and $D/d$= 8.33.

The simulations show that the flow and the temperature fields of the pulsating impinging jets have the similar general characteristics of the steady impinging jets at all instants of the period. As in the steady jet cases, the free jet region, the impingement region and the wall jet region form. In the steady jet case, there is no change in both temperature and velocity fields with time, however, when the jet is pulsating along the injection period, in all these regions, the velocity and temperature fields change in time. As a result, the jet renews itself continuously, and hence a higher heat removal rate from the hot bottom surface is expected in comparison with the steady impinging jet cases.

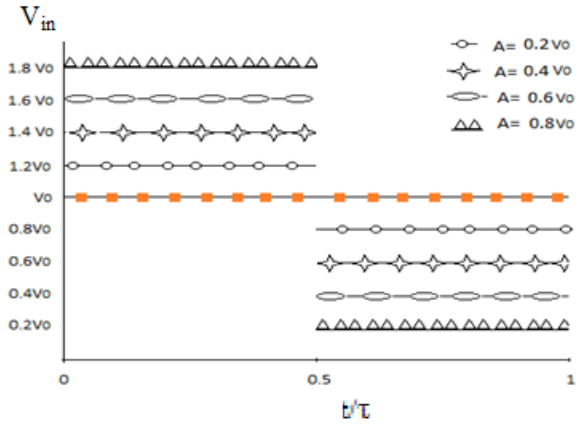


**Figure 2.** Variation of the jet velocity over a pulsation period.

The velocity vector distributions for the jets with Reynolds number 500, pulsation amplitude $A=0.2V_0$ and oscillation frequency of 1 *Hz* at four different instants of the period (t=0.0τ, 0.25τ, 0.5τ and 0.75τ) are shown in Fig. 3. In Fig. 4, the velocity vector distributions are shown for the jets with Reynolds number 500, pulsation amplitude $A=0.2V_0$ and pulsation frequency *f=3* Hz. Analysis of these figures shows that the flow fields exhibit the general behavior of a steady impinging jets. However, due to the pulsation of the jet velocity, secondary recirculating flow regions form and their location changes during the period.

In Fig. 3a, it is seen that in the beginning of the injection period (t=0.0τ), the ambient fluid entrains the free jet near the exit of the nozzle and a recirculating flow region forms. In time, as seen in Fig. 3 a, b, c and d, eye of the circulation moves towards the impingement point and then toward the outlet of the flow domain. As seen in these figures, the velocity vectors vary in the impingement region, more than other regions of the flow area. After hitting the plate, the flow accelerates again and starts to flow along the plate toward the exit. However, it is also seen that, in some parts, the fluid flows in the opposite direction, so that a number of circulations are formed. One circulation forms close to the free jet, and the other, within the wall jet region. The formation of these circulations can cause changes in heat transfer rate, thus, the secondary local maximums form in Nusselt number along the plate. Figure 3b depicts the flow field at the instant t=0.25τ of the pulsation period. The analogous descriptions about the flow field as the previous can also be drawn from this figure but, it is notable that the circulation formed have widened. Figure 3c and 3d show the flow field at two instants of the second half of the pulsation period. Considering the impingement region at all instants of the pulsation period, it can be seen that the magnitudes of the velocity vectors in the first part of the period are higher than those of the second part. This is an expected result, since the jet exit velocity in the first half of the period is higher than that in the second half.

Figure 4, shows the flow fields at the same instants of the pulsation period as in Fig. 3, for the case of *Re=500*, A= $0.2V_0$ and *f=3 Hz*. Comparison of velocity fields given in Figs 3 and 4 shows that with changing pulsation frequency from 1 to 3, the flow fields changes considerable as everything else is kept the same. As seen in these figures, in the impingement and wall jet regions, the flow field changes, more than all other parts of the flow domain so that two circulations form. There is also another circulations forming in the wall jet region. Another thing that should be pointed out is that two small eddies formed in the first half of the period merge and create a bigger circulation. The wall jet zone circulation also enlarges within the second half of the period, and becomes more obvious.

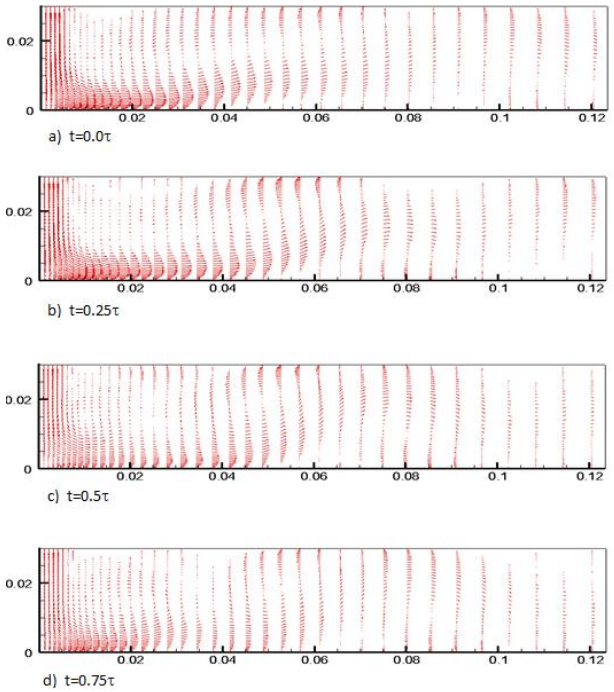


**Figure 3.** Velocity vector distributions at four different instants of pulsation period for *Re=500*, *A=0.2V₀* and *f=1 Hz*.

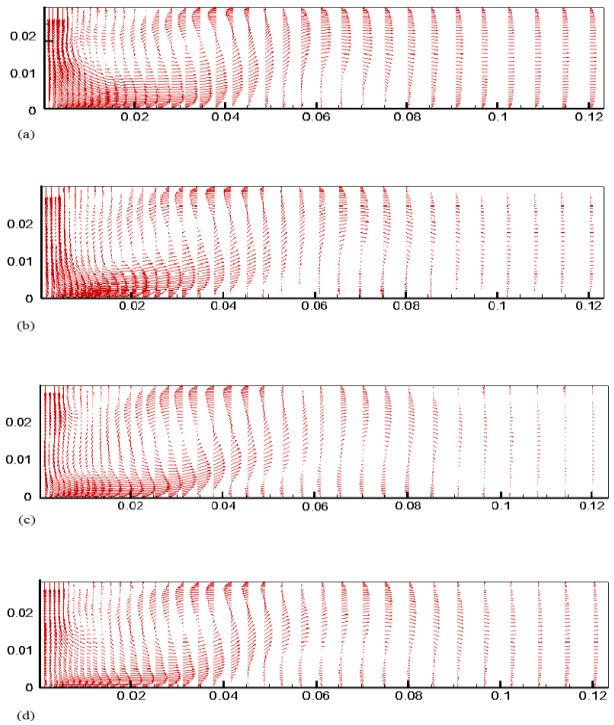


**Figure 4.** Velocity vector distribution at four different instants of pulsation period when *Re=500*, *A=0.2V₀* and *f=3 Hz*. a) *t=0.0 τ*, b) *t=0.25 τ*, c) *t=0.5 τ*, d) *t=0.75 τ*.

Figures 5 and 6 show the temperature fields at different instants of the pulsation period for the cases considered in Figs 3 and 4. It is seen in these figures that for both cases, the thermal boundary layer has its smallest thickness and the temperature gradients are very high around the impingement point. Hence, the heat transfer rate reaches its maximum value. This provides a means for efficient local cooling. It should be pointed out that

the boundary layer thickness increases toward the end of the injection period. This is the result of the variation of the jet exit velocity along the pulsation period.

To investigate the effects of Reynolds number, pulsation frequency and pulsation amplitude on the heat transfer rate from the bottom plate, the instantaneous local, time (period) averaged local, instantaneous stagnation point and period averaged stagnation point Nusselt numbers were calculated using Eqs. (7) through (11). Some of these results are discussed below.

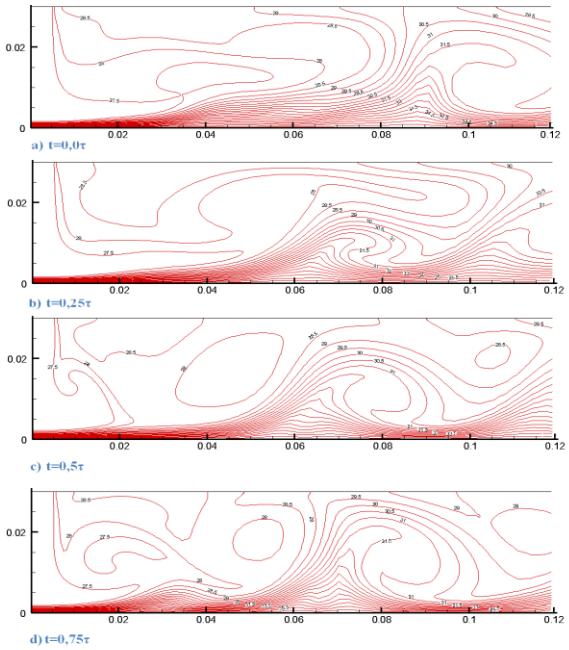


**Figure 5.** Temperature contours at four different instants of pulsation period when *Re=500, A= 0.2V₀* and *f=1 Hz.*

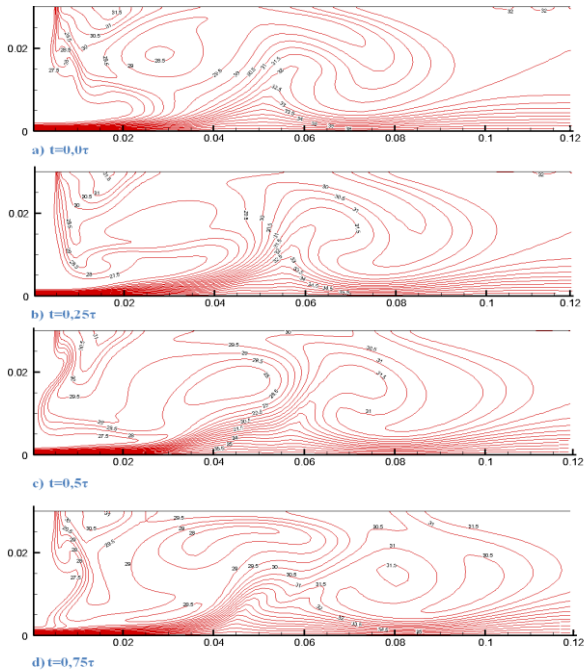


**Figure 6.** Temperature contours at four different instants of oscillation period when *Re=500, A= 0.2V₀* and *f=3 Hz.*

In order to see the variation of the heat transfer rate compared to that of the steady jet flow, Nusselt number variations along the bottom plate at different moments of the pulsation period were analyzed and compared with the steady jet Nusselt number. In this regard, in Fig. 7 the local Nusselt number variation curves over the bottom plate are given for two different amplitudes (*A= 0.4V₀* and *0.6V₀*) when *Re=500* and *f=2 Hz*. In Fig. 8, the similar results are given for *f=6 Hz*. In these figures, it is seen that the instantaneous Nusselt number curves are around the Nusselt number of the steady jet. Since the flow is pulsating, the impingement velocity of the fluid is different at different instants of the pulsation period. Hence, it is expected that the instantaneous Nusselt number changes with both position and time. Also, Nusselt number changes with both the pulsation amplitude and frequency. It is seen in Fig. 7 (a) and (b) that the highest stagnation point Nusselt number is attained at the instant *t= 0.375τ* in both cases shown in these figures. It is also seen that, at all instants of the period, Nusselt number curves have local maximum and minimum values at different locations. However, toward the exit of the flow domain, the Nusselt number curves at different instants converge to each other. Analysis of the results given in in Fig. 7 and 8 shows that at a given jet Reynolds number, the difference between steady jet Nusselt number and the pulsating jet Nusselt number increases with the increasing pulsation amplitude. With the increasing pulsation frequency, this difference decreases at all pulsation amplitudes.

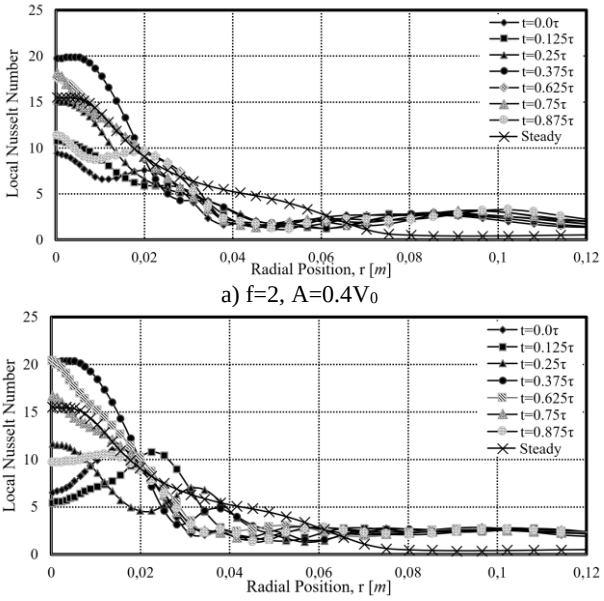


a) f=2, A=0.4V₀

b) f=2, A=0.6 V₀

**Figure 7.** Variation of instantaneous local Nusselt number along the bottom plate for Re=500 and oscillation frequency f=2 Hz at different oscillation amplitudes.

## CONCLUSIONS

In this study, pulsating impinging jets confined by two circular discs were considered. The bottom disc was kept at constant temperature, and the top disc was insulated. A pulsating air jet, issuing from a circular hole on the top

disc, was impinged on the bottom hot disc. The jet velocity was pulsated in time. A computer code based on control volume approach and SIMPLE algorithm was developed. The jet Reynolds number was varied between 100 and 700. The effects of the amplitude and frequency of the jet pulsation on the flow and temperature fields, and on the heat transfer rate from the bottom plate were numerically investigated.

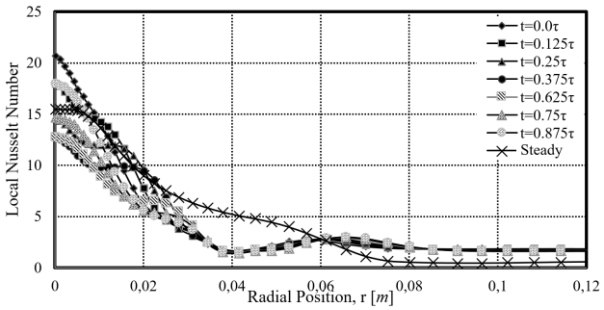


a) f=6, A=0.4$V_0$

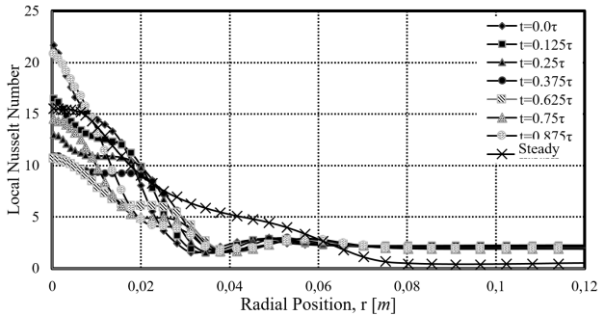


b ) f=6, A=0.6$V_0$

**Figure 8.** Variation of instantaneous local Nusselt number along the bottom plate for Re=500 and oscillation frequency f=6 Hz at different oscillation amplitudes.

It was observed that the general structures of the flow and temperature fields of pulsating jets are similar to the flow field of the steady jets. However, in the pulsating jet cases, circulating and moving flow regions form in the flow. These circulating flow regions become more apparent with increasing Reynolds number and pulsation amplitude.

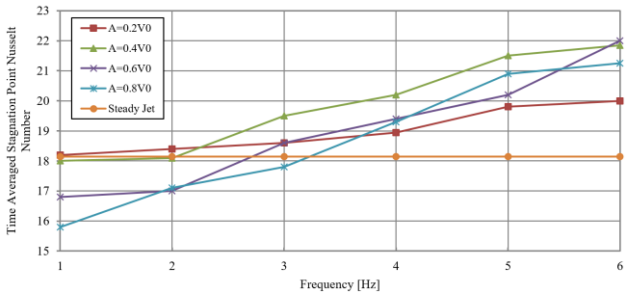


**Figure 9.** Period averaged stagnation point Nusselt number variation with the pulsation frequency and pulsation amplitude at *Re=700* and different.

At a given instant of the pulsation period, the local Nusselt number is maximum at the stagnation point and it decreases along the plate. This decrease in the local Nusselt number is not monatomic as in the steady jet case. It has local maximum and minimum values (fluctuations) due to the moving recirculating flow regions along the bottom wall. At low frequencies, the time (period) averaged stagnation point Nusselt numbers for all the pulsating jets considered are lower than the corresponding steady jet Nusselt numbers, However, with the increasing frequency, the stagnation point Nusselt number increases and become higher than the steady jet Nusselt number. With the increasing pulsation frequency, the impingement point Nusselt number increases up to a certain value of the frequency, after that value of the frequency, the impingement point Nusselt number approximately stays the same.

## REFERENCES


Azevedo, L. F. A., Webb, B.W. and Queiroz, M., 1994, Pulsed Air Jet Impingement Heat Transfer, *Exp. Thermal Fluid Sci.*, 8, 206–213.

Collucci, D. W. and Viskanta, R., 1996, Effect of Nozzle Geometry on Local Convective Heat Transfer to a Confined Impinging Air Jet, *Experimental Thermal and Fluid Science*, 13, pp. 71 – 80.

Demircan, T. and Turkoglu, H., 2010, The Numerical Analysis of Oscillating Rectangular Impinging Jets, *Numerical Heat Transfer, Part A*, 58, 146-161.

Goldstein, R. J. and Timmers, J. F., 1982, Visualization of Heat Transfer from Arrays of Impinging Jets, *International Journal of Heat and Mass Transfer*, 25, 1857 – 1868.

Goppert S., Gourtler T., Mocikat H. and Herwig, H., 2004, Heat Transfer Under a Precessing Jet: Effects of Unsteady Jet Impingement. *International Journal of Heat and Mass Transfer*, 47, 2795–2806.

Liu T. and Sullivan J.P., 1996, Heat Transfer and Flow Structures in an Excited Circular Impinging Jet, *Int. J. Heat Mass Transfer* 39 (17), 3695–3706.

Miladin, E.C. and Zumbrunnen, D. A., 1997, Local Convective Heat Transfer to Submerged Pulsating Jets, *Int. J. Heat Mass Transfer*, 40 (14), 3305–3321.

O'Donovan T. S. and Murray. B., 2008, Fluctuating Fluid Flow and Heat Transfer of an Obliquely Impinging Air Jet, *International Journal of Heat and Mass Transfer*, 51, 25-26.

Poh H. J, Kumar K. and Majumdar A. S., 2005, Heat transfer from a pulsed laminar impinging jet, *International Communications in Heat and Mass Transfer*, 32, 1317–1324.

Zumbrunnen, D. A. and Aziz, M., 1993, Convective Heat Transfer Enhancement Due to Intermittency in an Impinging Jet, *J. Heat Transfer*, 115 91–98.